

Screen printing to create 3D tissue models

*Narendra Pandala, Sydney Haywood, Michael A. LaScola, Adam Day, Joshua Leckron, Erin Lavik**

Chemical, Biochemical and Environmental Engineering, University of Maryland, Baltimore County, MD 21250, Piscataway Territories

*corresponding author, elavik@umbc.edu

KEYWORDS: screen printing, *in vitro* models, bioprinting, layered printing, 3D models

ABSTRACT: 3D printing has revolutionized making tissue models, but the instruments are often quite expensive, and the approach can involve heat and/or shear forces that can damage cells. As a complement to more traditional 3D printing approaches, we looked at screen printing. Screen printing is an additive manufacturing technique used to pattern inks through screens supporting patterns onto different surfaces. It has a wide range of applications ranging from traditional printing to printing electric circuit boards. Taking cues from this we have developed a process of screen printing live cells along with a suitable scaffold on to different surfaces to generate *in vitro* models. The process is not only inexpensive and simple to use, but it also offers a wide range of advantages like the ability to use a range of bioinks limited only by their gelation time, printing on different surfaces, and the ability to autoclave all of the major components. In this paper, we

present the screen assembly and the setup we used to print the cells along with the resolution and limits of features printed and the effect of the printing on the cells.

INTRODUCTION

3D printing as an additive manufacturing technique has been quickly developing since its inception in the 1990's¹. Apart from its uses starting from rapid prototyping to manufacturing various machine parts, it is also used in tissue engineering²⁻³. Similar to traditional 3D printing, 3D bioprinting is an additive process by which layers of cells and scaffolds are deposited on to a surface by various methods such as Needle Extrusion Bioprinting, Inkjet Bioprinting, and Laser Assisted Bioprinting.^{2, 4} In 3D bioprinting cells are printed in layers building more complex three dimensional architectures³, this opens the door for vastly improved *in vitro* models, which provide a critical starting point for drug screening and understanding cellular mechanisms corresponding to different conditions⁵.

3D bioprinting has many advantages in creating models of tissues and organoids *in vitro* which are a better mimic of the tissue or organ². Also, 3D bioprinting has a huge potential for developing organs for transplant. Even though 3D bioprinting has a huge potential, the cell viability in the printed structures is very much dependent on the type of process, extrusion technique, any thermal variations, the bioink used, and the cell physiology, which results in a range of viabilities⁶⁻⁷. Other than this many bio printing strategies have their own set of drawbacks depending on the technique used for printing, also in some cases, the bioprinting strategies result in phenotypic changes in the cells which might not be desirable^{2, 8-9}. The printing time of bioprinting also depends on the gelation time of the bioink and the technique

implemented which is also detrimental in the cell viability and growth³. Other than 3D bioprinting techniques including spheroids¹⁰, scaffolds¹¹, microplates, and microfluidic devices¹² have been used to create 3D *in vitro* models which better mimic the *in vivo* environment than traditional 2D *in vitro*¹³.

To overcome some of the drawbacks of 3D bioprinting and to create a simple process of creating 3D *in vitro* models at a small scale with a variety of bioinks and cells we developed a process based on the traditional lithographic screen printing. In this paper, we demonstrate a screen-printing technique to generate 3D *in vitro* models in a high throughput fashion. Screen printing has been used in lithography and calligraphy for over 1000 years and has been established as a widely used technology compared to the other printing methods because of its low cost and its adaptability to change.¹⁴ In recent years screen printing has been employed in the electronics industry to print layers of conductive and resistive materials onto printed circuit boards¹⁵⁻¹⁶, to print sensors on different surfaces¹⁷⁻²¹, as an additive manufacturing technique to create 3D structures²², and to construct microfluidic devices²³⁻²⁴. Apart from this, screen printing is used in synthetic biology to spatially control the growth of bacteria on different surfaces²⁵.

Based on this, we have developed a 3D screen printing process that allows for the creation of 3D structures using hydrogels containing live cells, allowing for the development of 3D cultures. The screen printing process offers several advantages in constructing tissue scaffold, like the materials required to make screens are very inexpensive and the screens can be sterilized using an autoclave making them usable in a laminar flow hood in an aseptic fashion, also a wide range of viscosities can be used in printing making it compatible with a large number of bioinks. The screen printing process can also be used to print patterns of cells with hydrogel scaffolds on to multiple surfaces in a high throughput fashion making it a good option to screen drugs. This

paper provides a proof of concept that screen printing is a straightforward technique that can be used to develop 3D cell cultures with ease. This paper also presents the process of screen printing, the resolution of features obtained using the process, and the effect on the cells.

RESULTS

Screen assembly, printing process and durability

The process of multilayered screen printing on a hydrogel surface is shown in Figure 1. The process of screen printing begins with the assembly of screens, this process is not only inexpensive but also does not require any specialized equipment (Supplementary Figure 1). The screens used are constructed using a reinforced wooden frame and a silkscreen, with a water-resistant emulsion making them a cost effective way (each screen costing around 10 USD) of printing hydrogel scaffolds for cells. The water-resistant emulsion along with the reinforced wooden frame makes the cleaning of the screens easy. The screens can be sterilized using an autoclave, which makes them suitable to be used in an aseptic process (Supplementary Figure 2). For this paper, we are focusing on the use of gelatin, but any material that gels in approximately 3-10 minutes works well with the process. Materials that gel faster than 3 minutes require working extremely rapidly, and those that gel slower than 10 minutes risk losing the resolution of the printing process. Once the gelatin or the hydrogel components set into the required pattern, the coverslips can be placed in a well plate and growth media can be then added on top of the coverslips or the glass slides with the pattern for the cells to grow in.

We observed that the screens can be washed, sterilized, and reused over 30 times, before noticing the wear and tear in the minute details of the hardened emulsion, and loss of tension in the mesh. The screens can also be recycled by removing the emulsion coating using ethanol and reapplying a new coat of sensitized emulsion and photomasking new patterns.

The process of screen printing can be used in combination with multiple types of inks with varying viscosities and other properties, for example, the electronics industry uses various conductive and resistive and photosensitive inks with widely ranging properties²⁶⁻²⁷, this makes the screen printing process readily usable with a range of bioinks, supplemented with various ECM proteins and other media components with a minimum amount of tweaking to the process. Additionally, the screen printing process can be used to print a wide range of substrates ranging from absorbent materials like paper, cloth used in traditional lithography to non-absorbent surfaces like glass, metal, ceramics, and plastic circuit boards²⁷, this makes the screen printing process easily adaptable to print on various materials like ranging from semi-permeable membranes to glass slides and coverslips or other substrates based on the user requirement.

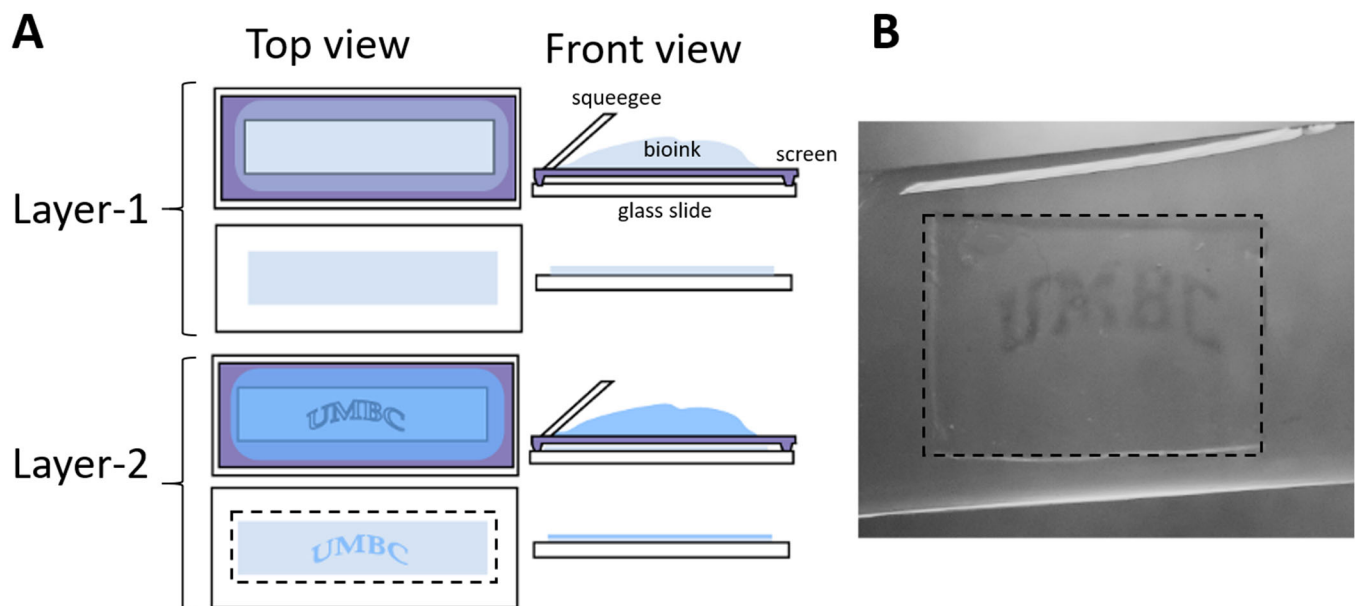


Figure 1. (A) Schematic of screen printing process with hydrogels and showing patterning for two layers. (B) Multilayered print as proof of principle, a hydrogel containing dye was screen printed on another layer of hydrogel with a UMBC patterned screen.

Resolution testing

To test the resolution of the screen printing process, we started with three different patterns at varying sizes. Since the mesh size of the screens is 125 μm , we began testing out starting at double the mesh size to create reliable patterns on the screens. Even though feature sizes between 250 μm and 400 μm can be photomasked onto screens and printed, the ease of making the screens and the reproducibility was an issue at this size. This is was mainly due to the resolution limit of an inkjet printer, which makes the individual features overlap on the transparent sheet and the difficulty in washing the small features when transferred on the emulsion coated silkscreen due to the rapid photo hardening of the emulsion in the minute details in the patterns. So patterns with features having a thickness starting from 400 μm , which had much greater reproducibly and reliability were used in resolution testing. Since all patterns can be constructed as a combination of lines, curves, and dots, we chose a set of parallel lines, a set of concentric circles, and a set of dots of varying sizes for resolution testing. A 10% w/vol solution of gelatin at 35°C is used as the bio ink in printing these structures. The size of the patterns on the transparent sheet (the diameter of the dots, the thickness of the lines and the concentric circles) showed an average difference of the 75 μm from the sized programmed to print in the Adobe Illustrator (Supplementary Figure 3). These assembled screens are used to print patterns using a

20 μ l volume of 10% w/vol gelatin solution on to a clean glass slide and then the dimensions of these printed patterns are then measured. Figure 2A-E shows the height heat maps of the features at a range of magnifications.

From that data, it can be observed that the small structures (below 500 μ m) have an inflated size and the larger structures (above 500 μ m) have a reduction in the dimensions (Figure 2F). Even though there is a very small disparity of an average of 90 μ m in the sizes of the patterns printed, from the intended size of the print, this does not affect the shapes of the pattern, i.e. all the minute details in the pattern are transferred on the print with only a slight difference in size, but not the shape of the pattern (Figure 2C-E). This size difference in the pattern is due to the initial stages of the transparent sheet printing (Supplementary Figure 3) which can be fixed by adjusting the sizes in the Illustrator to obtain more accurate sizes in the final structures. Also, it can be noted that very fine details from the screen are transferred onto the prints. Using the three-dimensional heatmaps of the scanned prints the heights of the prints are obtained (Figure 2G). The height varies from 1 μ m to 4 μ m of the individual structures. This height of the structures can be manipulated to an extent by printing layers on top of each other creating a 3D structure for the cells to grow in.

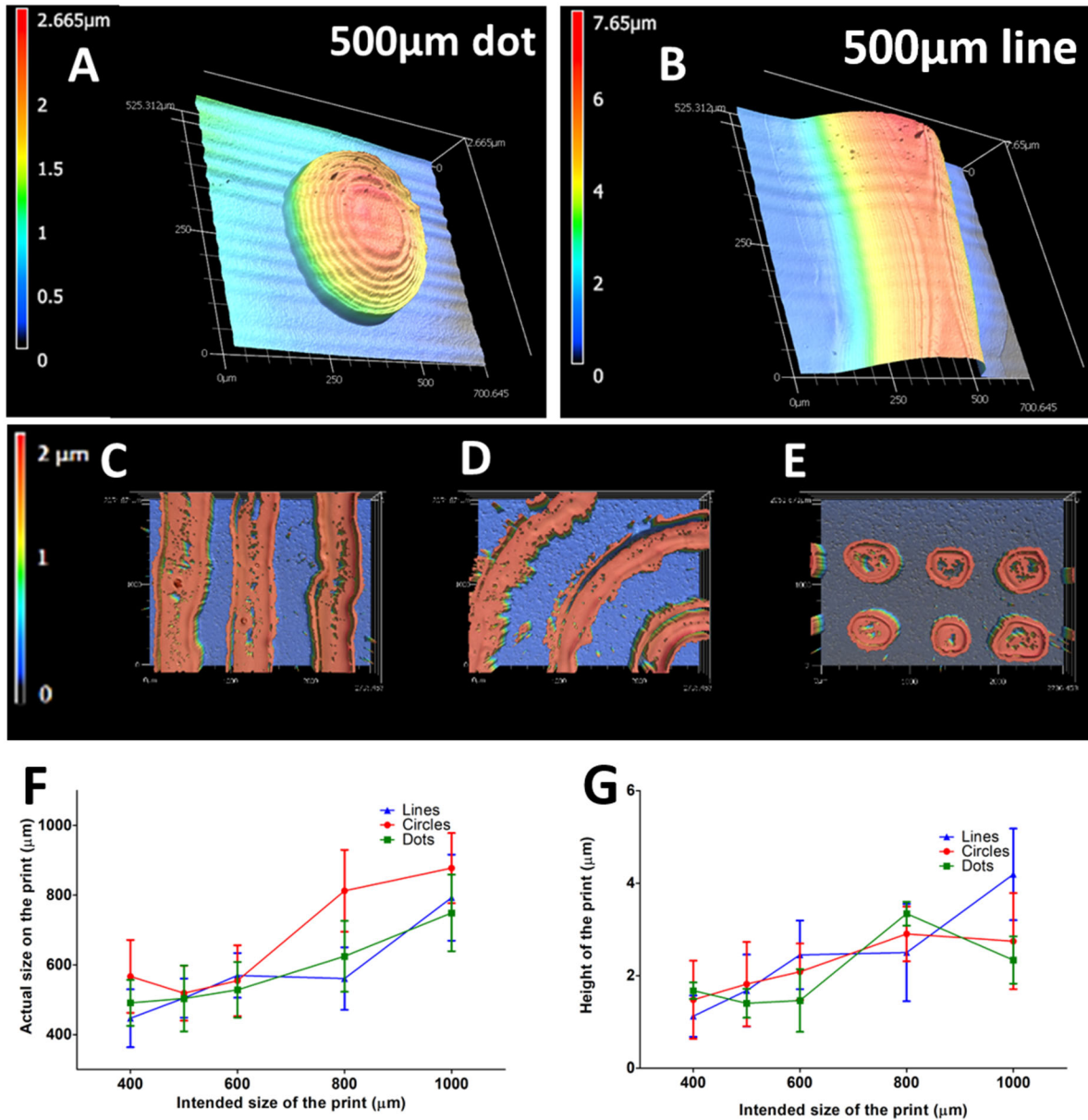


Figure 2. Heat map of a feature (A) one dot of 500μm diameter size in a grid of dots(20x, n=3) (B) part of a line 500μm thick in a set of lines(20x , n=3); Set of (C) parallel lines (D) concentric circles (E) dots printed using 10%w/vol gelatin solution as the bioink in the screen printing process(5x, n=6); Resolution data of the (F) size and (G) height of the features; A set of 3 prints per size per pattern have been taken and 6 images at 5x resolution was used to measure the x-y dimensions and 3 images at 20x resolution were used to collect the height data.

Multilayered printing

To print a wider variety of structures and also to accommodate multiple cell types and different bioinks, we used the screen printing process to print multiple layers on top of each other. For this we chose a crosshatch pattern obtained by using the set of parallel lines printed on top of each other (Figure 3A-B). To observe the increase in height of the structure a first layer is printed, and the height of this layer is measured and then a second layer is printed perpendicularly on top of the first and the height of the structure is measured. From the height analysis of the two layers it can be observed that the height of the structures is increased by adding a second layer (Figure 3C), which serves as an indication that more complex patterns can be obtained by multilayered printing. To add to this, we have printed a smaller dot pattern on top of larger diameter dots. A dot pattern of 250 μm size is printed above a 600 μm dot pattern and the aligned dots are imaged and analyzed. Figure 3D shows the heatmap of the multilayered dot print and Figure 3E shows the height profile of the print. From the heatmap and the height profile, it can be noted that the height of the feature can be increased by adding layers of prints. This serves as an indication that the height of prints in the screen printing process can be increased by adding layers on top of each other and also that this process can be used to encapsulate multiple cell types and different bioinks to produce complex patterns, with varying height in a simplistic fashion.

Traditionally screen printing has been used to print a few thin layers of inks either on top of each other or aligned on the side of each other to print the required pattern. Here in this paper, we demonstrate that both of these can be done manually to achieve a complex pattern composed of various bioinks and multiple layers. Using this manual process 3-4 layers can be easily printed, on top of each other, but this process can be automated to add more layers to create much complex structures.

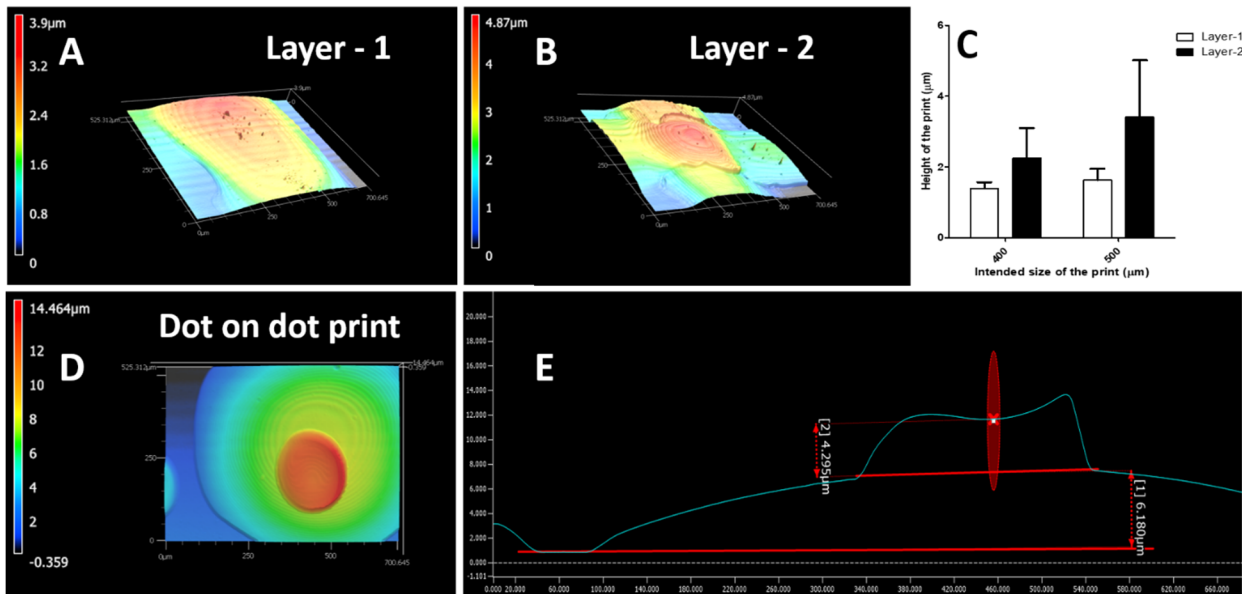


Figure 3. Heatmaps, showing multilayered printing of (A) the first layer of 400 μm lines (20x) and (B) the second layer of the 400 μm (20x) (C) Height data of multilayered prints constructed using 400 μm and 500 μm width series of lines (D) heat map of the aligned dots of 200 μm on top 600 μm dots (20x) and (E) the height profile of the multilayered feature showing an increased height; A set of 3 prints per pattern per size were taken and all the dimensions were measured at 20x magnification.

Effect of the printing on the cells

Colorectal adenocarcinoma cells (Caco-2) were used to test the effect of the printing process on cell survival. To test the effect of the screen printing process on the cells, Caco-2 cells are mixed with 10% w/vol gelatin solution and printed onto coverslips and then live/dead assays were used to visualize and measure the viability of the cells. Figure 4A-B shows the live dead images of the Caco-2 and the gelatin bioink printed onto a glass slide using a 500 μm line pattern and cells in the just the Caco-2 and the gelatin mixture as a control. To further quantify the cell survival during the screen printing process and to compare it to the viability of the cells passed

through a 30G needle, cells were printed using a 125um screen, extruded through a 30G needle using culture media and gelatin as the bioink (Figure 4C, Supplementary Figure 4). From the data it can be observed that screen printing the cells using gelatin as the bioink has similar viability as the control (Figure 4C). The cells printed using just the mixture of cells and media have shown a decreased viability compared to the other conditions, this might be due the direct exposure of cells to the sheer of squeegee and the screen, this can be easily avoided by using a suitable bioink, which can be observed in the gelatin cell prints which show as similar viability as the control. So, this process can be used to print live cells into structures using suitable bioinks to generate 3D *in vitro* models.

It is known that the stresses involved during bioprinting can result in cell damage, reduction in cell viability and also phenotypic changes in some cases⁹. Since the cells passing through the screen printing process experience the stress only for a few seconds while passing through the screen, we assessed the effect of this process immediately after the printing. From the results it was observed that with the use of a scaffold the cells experience no significant damage in comparison to control.

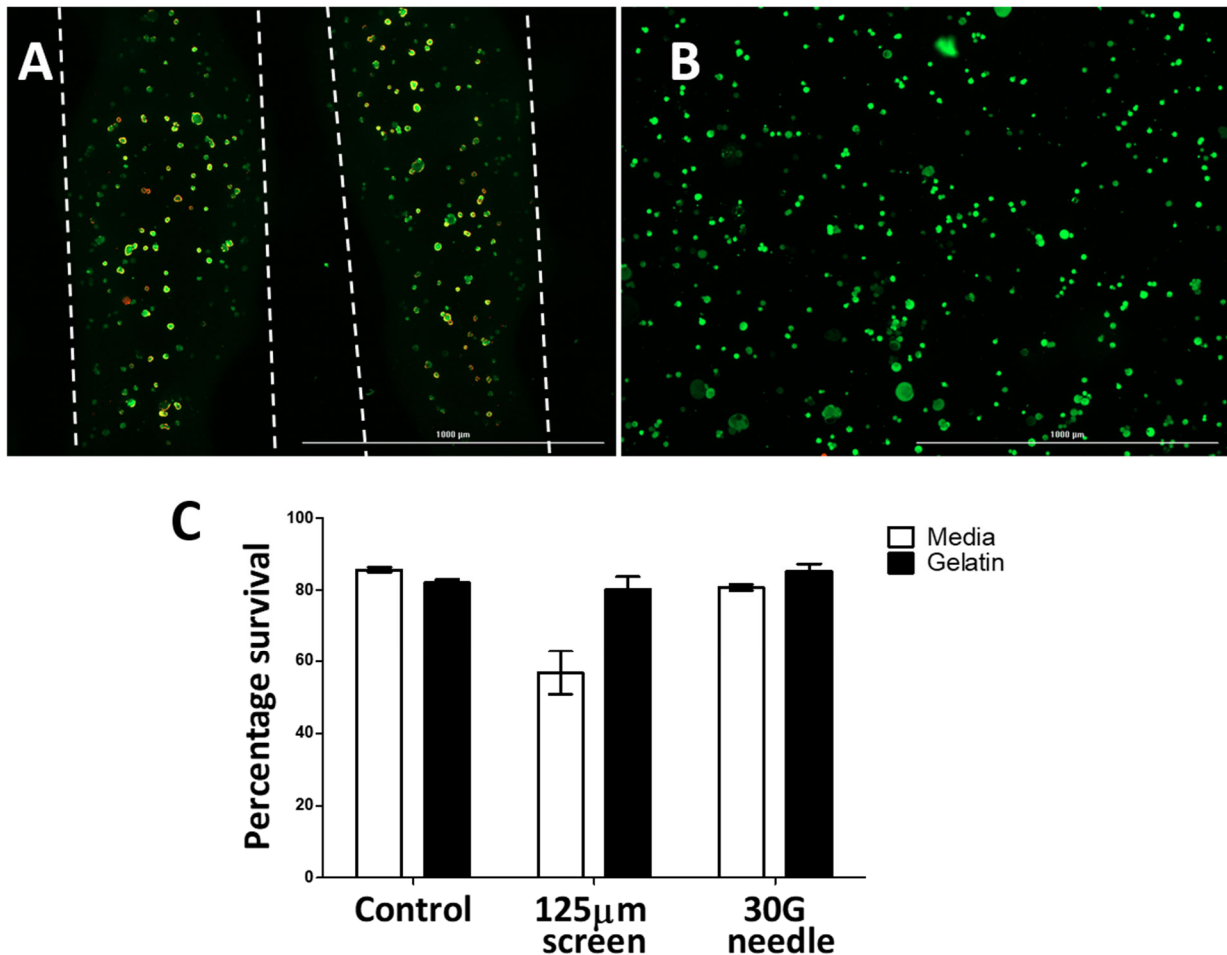


Figure 4. (A) Fluorescent of images of Caco-2 cells A) printed using a 125 μm mesh size with a 500 μm line pattern and B) media control stained using calcein-AM (green) the live cells and ethidium homodimer-1(red) for the dead cells (C) Viability of the Caco-2 cells printed using a screen of 125 μm mesh size along with the control and a 30G needle (n=4)

DISCUSSION

In this paper we created a completely manual process which can be easily reconstructed without the requirement of any specialized equipment and which can be used in an aseptic fashion for mammalian cells, but also this process can be augmented by higher rigidity scaffolds or automation or different substrates to create a much more complex plethora of models. The

resolution of the screen printing process can also be increased by using finer mesh screens, tweaking the emulsion formulations, and using high resolution photomasks, we chose a $125\mu\text{m}$ mesh size screen in order to accommodate for the mammalian cells without getting obstructed by the screen, a commercially available emulsion and an inkjet printer for printing the photomasks to keep the process easily reproducible. 3D bioprinters are used to print features of varying size ranging from $10\mu\text{m}$ to $1000\mu\text{m}$ ²⁸⁻²⁹ depending on the cell type and application for example a resolution of around $200\mu\text{m}$ is found to be suitable for blood vessels and organoids³⁰, a finer resolution of $50\mu\text{m}$ is needed to print cell laden microfluidic devices³¹, and a much less demanding resolution of around $500\mu\text{m}$ is needed to construct renal tubes³². The screen printing process could easily be used to print the structures of similar resolution with ease, to create these models. Also, it can be noted that we have used glass slides to test the resolution of the screen printing process for the purpose of imaging, there can be a slight spreading or absorption of the bioink when using a permeable or semi permeable substrate which needs to be tuned to achieve the optimal setup for each application. In this paper we developed a simple process similar to traditional lithographic screen printing technique to print thin structures of gelatin, but with automation, and gels with the right structural rigidity and binding properties a 3D structure which a higher level of complexity and height can be generated like the 3D screen printing process^{22, 33}.

Resolution of the features is an important factor for any printing process. Depending on the mechanism of crosslinking of the hydrogel, predominantly and whether the gel is synthetic or naturally derived the resolution of bioprinting varies with a much finer resolution with the synthetic gels and a relatively coarser resolution with the naturally derived hydrogels³⁴. Recently, much finer resolution of around $20\mu\text{m}$ has been achieved even by using naturally derived

hydrogel like collagen, but this comes at a cost of extruding the cells separately, and not along with the collagen, since the collagen has to be acidified and printed onto a pH-buffered support bath to achieve a fine resolution³⁵. Also, it has been shown the encapsulating cells within the hydrogel (gelatin) can lower the resolution of the printing process³⁶. Screen printing being an analog process supporting a wide range of inks from a thick paste to a gelatinous liquid in a short span of time, can be used as a potential technique to print small sized *in vitro* models with various cell type, bioinks in a quick way.

The resolution of the features achieved by the screen printing technique can be as fine as 50µm with a very precise margin^{26, 37-38}. For the purpose of this paper we chose to create a simplistic manual process, without the need of specialized equipment which can be easily replicated, from this process we developed patterns of the order of 100µm which is very much comparable to that of the 3D bioprinting techniques³¹.

We quantified the effect of the screen printing process on the cells and found no significant damage to the cells compared to the cells extruded by needed or the control with the use of a suitable bioink. Unlike traditional bioprinters which sometimes experience a thermal variation or a long extrusion channel for a significant amount of time, the screen printing process is very quick *i.e.* the time the cells are passed through the screen or experience any stress is 1 or 2 seconds which might help in reducing cell damage and may not present any phenotypic changes. This can be supported by the viability of the cells using the gelatin scaffold, but further testing on multiple cell types at different time points after the printing is needed to accurately determine the effect of this process on the cells.

Screen printing has been used for thousands of years, and it has applications in fields as diverse as art and electronics. The power of the technique is that it allows one to combine multiple kinds of approaches. One can screen print on a wide range of materials from cloth to scaffolds to silicone, and one has the potential to integrate electronics into the system. The question we had was whether we could print mammalian cells and their synthetic extracellular matrix in this system, if so, we would have the possibility of being able to leverage the vast experience and range of materials associated with the technique. The work here demonstrates that not only can we print mammalian cells and their extracellular matrix or hydrogel systems, but we can do so reproducibly, with good resolution and cell viability.

CONCLUSIONS

The screen printing process is a simple approach to build 3D tissue models. All the materials required for the screens can be easily procured and constructed without the use of any specialized equipment at very low cost with each screen costing less than 10 USD. The small footprint of the screens and the fact that they can be easily sterilized make them easy to incorporate in an aseptic process. While we have focused here on gelatin on glass, the process is amenable to printing on a range of surfaces from membranes to degradable materials and can be combined with other 3D printing techniques to build out models. One of the other attractions is that one can print multiple replicates in parallel with the system. Given the simplicity of the process, the time to print a model, and the ability to print multiple patterns make this a promising technology to print multiple patterns in a short time for high throughput screening. The resolution data acquired from the set of three prints, per size, per pattern indicates that the screen printing process is very consistent and reproducible. Even though there is a slight margin of error in the intended size of the print compared to the actual size of the print, the shape of the pattern

holds very well making the prints suitable for use in developing *in vitro* models. The slight variation in prints is due to the intermediate steps involved in transferring the print from the digital version on to the screen and can be easily fixed by accounting the prints from the inkjet printer. Printing layers on top of each other cannot only be used to increase the size of structures but also can be used to layer multiple cell types or bioinks on top of each other, creating complex structures to understand the interactions between the various types of cells or similar cells in different bioinks. The live dead data suggests that the screen-printing process is equivalent to other 3D printing approaches for cell viability, and the simplicity, cost, and ease of use make the approach an important tool for making 3D tissue models.

MATERIALS AND METHODS

Screen assembly

The screens used are constructed using a wooden frame of size 4"x6" reinforced with staples over which a tightly stretched silkscreen of mesh size 125 μ m (43T, 110US) is attached. A water-resistant photosensitive diazo emulsion Ulano-925WR-P (New York, USA) is then sensitized according to the manufacturer's instructions and a thin layer of the sensitized emulsion is coated on to the stretched silkscreen and the screen is dried in a dark place overnight. The pattern of interest is designed using Adobe Illustrator and is printed on a transparent sheet in saturated black using an inkjet printer. This pattern is placed on the silkscreen with the dried emulsion coating and exposed to UV light for approximately 3 minutes. This results in the hardening of the exposed areas of the screen and the unexposed pattern is washed away with a water spray. The screen is dried under white light for an hour and then sterilized in an autoclave.

Printing Process

A clean slide or a coverslip or hydrogel surface on to which the desired pattern is to be printed is placed below an aluminum foil collar and the screen is placed on top of the collar such that the pattern is above the slide. The required volume of gelatin or the hydrogel components mixed together with the cells and extracellular matrix proteins (ECM) are placed next to the pattern on the screen and an aluminum squeegee (3"x3") is used to push the hydrogel components or the gelatin through the screen on to the surface of the slide. In this paper, a 10% w/vol solution of gelatin at 35°C is used as the bioink which when printed on the glass slide sets into a hydrogel.

Imaging and Analysis

A 3D laser scanning confocal microscope VK-X1000 (Keyence, Japan) is used to image the prints and the Multifile analyzer software (Keyence, Japan) is used to analyze the images and measure the sizes of the patterns and structures obtained during the screen assembly and printing process. Three prints of each size and shape are taken, for each print six images are taken at 5X magnification to measure the horizontal dimensions of the prints and three images are taken at 20X magnification to measure the height of the prints. The diameters of the dots and the thickness of the lines and concentric circles of the printed structures are then measured using the plane measurement functions in the multifile analyzer software and the vertical profile of the features are measured by using the profile function, and then the average height is calculated using the area under the profile curve and the horizontal thickness of the feature.

Cells and Live/Dead Assay

Caco-2 cells obtained from ATCC, USA were cultured using MEM alpha supplemented with 20% Fetal bovine serum. 10,000 cells were mixed with either culture media or 20 μ l of 10% w/vol gelatin solution and then printed using screen printing process. Then the printed cells are stained using 4 μ M of calcein-AM as live stain and 8 μ M of ethidium homodimer-1 as dead stain.

Imaging and Population Analysis:

The cells and the cells in the screen printed scaffolds were then imaged using a live cell imaging multimode reader (Cytation 5, Biotek, USA). To quantify the data of the live dead assays a laser scanning fluorescence microplate cytometer (Acumen, TTP Labtech, UK) and the data is analyzed by using the cellista software (TTP Labtech, UK). The Acumen uses the High content screening technique³⁹ to analyze the microplate assays and here the program is set to detect the population of the live and dead cells in each cohort.

ASSOCIATED CONTENT

Supporting Information.

Supplementary Figure 1. Detailed screen assembly protocol. Supplementary Figure 2. Sterilizing the screen printing setup; Supplementary Figure 3. Sizes of the prints on the transparent sheets used for photomasking. Supplementary Figure 4. Live dead scans of screen printed cells.

AUTHOR INFORMATION

*** Corresponding Author**

Erin Lavik

Email: elavik@umbc.edu

Funding Sources

This work is financially supported by National Science Foundation (Award No. 1804743) and by Maryland Stem cell research fund (2019-MSCRFD-5064).

Notes

The authors declare the following competing financial interest: A. Day and E. Lavik are inventors on a patent involving the technology, and E. Lavik is a founder of Ortuvu LLC that has licensed the technology.

REFERENCES

1. Hull, C., StereoLithography: Plastic prototypes from CAD data without tooling. *Modern Casting* **1988**, *78* (8), 38.
2. Murphy, S. V.; Atala, A., 3D bioprinting of tissues and organs. *Nat Biotechnol* **2014**, *32* (8), 773-85.
3. He, Y.; Yang, F.; Zhao, H.; Gao, Q.; Xia, B.; Fu, J., Research on the printability of hydrogels in 3D bioprinting. *Sci Rep* **2016**, *6* (1), 29977.
4. Guvendiren, M.; Molde, J.; Soares, R. M.; Kohn, J., Designing Biomaterials for 3D Printing. *ACS Biomater Sci Eng* **2016**, *2* (10), 1679-1693.
5. Justice, B. A.; Badr, N. A.; Felder, R. A., 3D cell culture opens new dimensions in cell-based assays. *Drug discovery today* **2009**, *14* (1-2), 102-7.
6. Zhang, T.; Yan, K. C.; Ouyang, L.; Sun, W., Mechanical characterization of bioprinted in vitro soft tissue models. *Biofabrication* **2013**, *5* (4), 045010.
7. Yu, Y.; Zhang, Y.; Martin, J. A.; Ozbolat, I. T., Evaluation of cell viability and functionality in vessel-like bioprintable cell-laden tubular channels. *Journal of biomechanical engineering* **2013**, *135* (9), 91011.
8. Gungor-Ozkerim, P. S.; Inci, I.; Zhang, Y. S.; Khademhosseini, A.; Dokmeci, M. R., Bioinks for 3D bioprinting: an overview. *Biomaterials science* **2018**, *6* (5), 915-946.
9. Ning, L.; Betancourt, N.; Schreyer, D. J.; Chen, X., Characterization of Cell Damage and Proliferative Ability during and after Bioprinting. *ACS Biomaterials Science & Engineering* **2018**, *4* (11), 3906-3918.
10. Hamamoto, R.; Yamada, K.; Kamihira, M.; Iijima, S., Differentiation and proliferation of primary rat hepatocytes cultured as spheroids. *Journal of biochemistry* **1998**, *124* (5), 972-9.
11. Edmondson, R.; Broglie, J. J.; Adcock, A. F.; Yang, L., Three-dimensional cell culture systems and their applications in drug discovery and cell-based biosensors. *Assay Drug Dev Technol* **2014**, *12* (4), 207-218.
12. Toh, Y. C.; Zhang, C.; Zhang, J.; Khong, Y. M.; Chang, S.; Samper, V. D.; van Noort, D.; Hutmacher, D. W.; Yu, H., A novel 3D mammalian cell perfusion-culture system in microfluidic channels. *Lab on a chip* **2007**, *7* (3), 302-9.
13. Fernandes, D. C.; Canadas, R. F.; Reis, R. L.; Oliveira, J. M., Dynamic Culture Systems and 3D Interfaces Models for Cancer Drugs Testing. *Advances in experimental medicine and biology* **2020**, *1230*, 137-159.
14. Travis, T., A history of screen printing: how an art evolved into an industry. Guido Lengwiler. Cincinnati, OH: ST Media Group International, 2013. 484 p. ill. ISBN 9780944094747 \$75.00 (hardcover). *Art Libraries Journal* **2016**, *41* (1), 65-67.
15. Suikkola, J.; Björninen, T.; Mosallaei, M.; Kankkunen, T.; Iso-Ketola, P.; Ukkonen, L.; Vanhala, J.; Mäntysalo, M., Screen-Printing Fabrication and Characterization of Stretchable Electronics. *Sci Rep* **2016**, *6* (1), 25784.
16. Kim, Y. D.; Hone, J., Screen printing of 2D semiconductors. *Nature* **2017**, *544* (7649), 167-168.
17. Nomura, K. I.; Horii, Y.; Kanazawa, S.; Kusaka, Y.; Ushijima, H., Fabrication of a Textile-Based Wearable Blood Leakage Sensor Using Screen-Offset Printing. *Sensors (Basel, Switzerland)* **2018**, *18* (1), 240.
18. Zhu, C.; Chortos, A.; Wang, Y.; Pfattner, R.; Lei, T.; Hinckley, A. C.; Pochorovski, I.; Yan, X.; To, J. W. F.; Oh, J. Y.; Tok, J. B. H.; Bao, Z.; Murmann, B., Stretchable temperature-

sensing circuits with strain suppression based on carbon nanotube transistors. *Nature Electronics* **2018**, *1* (3), 183-190.

19. Cao, R.; Pu, X.; Du, X.; Yang, W.; Wang, J.; Guo, H.; Zhao, S.; Yuan, Z.; Zhang, C.; Li, C.; Wang, Z. L., Screen-Printed Washable Electronic Textiles as Self-Powered Touch/Gesture Tribo-Sensors for Intelligent Human-Machine Interaction. *ACS nano* **2018**, *12* (6), 5190-5196.
20. Lamas-Ardisana, P. J.; Martínez-Paredes, G.; Añorga, L.; Grande, H. J., Glucose biosensor based on disposable electrochemical paper-based transducers fully fabricated by screen-printing. *Biosensors & bioelectronics* **2018**, *109*, 8-12.
21. Albareda-Sirvent, M.; Merkoçi, A.; Alegret, S., Configurations used in the design of screen-printed enzymatic biosensors. A review. *Sensors and Actuators B: Chemical* **2000**, *69* (1), 153-163.
22. Dressler, M.; Studnitzky, T.; Kieback, B. In *Additive manufacturing using 3D screen printing*, 2017 International Conference on Electromagnetics in Advanced Applications (ICEAA), 11-15 Sept. 2017; 2017; pp 476-478.
23. Juang, Y.-J.; Li, W.-S.; Chen, P.-S., Fabrication of microfluidic paper-based analytical devices by filtration-assisted screen printing. *Journal of the Taiwan Institute of Chemical Engineers* **2017**, *80*, 71-75.
24. Liu, M.; Zhang, C.; Liu, F., Understanding wax screen-printing: A novel patterning process for microfluidic cloth-based analytical devices. *Analytica Chimica Acta* **2015**, *891*, 234-246.
25. Moon, S.; Fritz, I. L.; Singer, Z. S.; Danino, T., Spatial Control of Bacteria Using Screen Printing. *3D Print Addit Manuf* **2016**, *3* (4), 194-203.
26. Hyun, W. J.; Lim, S.; Ahn, B. Y.; Lewis, J. A.; Frisbie, C. D.; Francis, L. F., Screen Printing of Highly Loaded Silver Inks on Plastic Substrates Using Silicon Stencils. *ACS applied materials & interfaces* **2015**, *7* (23), 12619-24.
27. Faddoul, R.; Reverdy-Bruas, N.; Blayo, A., Formulation and screen printing of water based conductive flake silver pastes onto green ceramic tapes for electronic applications. *Materials Science and Engineering: B* **2012**, *177* (13), 1053-1066.
28. Bajaj, P.; Schweller, R. M.; Khademhosseini, A.; West, J. L.; Bashir, R., 3D biofabrication strategies for tissue engineering and regenerative medicine. *Annual review of biomedical engineering* **2014**, *16*, 247-76.
29. Mandrycky, C.; Wang, Z.; Kim, K.; Kim, D. H., 3D bioprinting for engineering complex tissues. *Biotechnology advances* **2016**, *34* (4), 422-434.
30. Miri, A. K.; Nieto, D.; Iglesias, L.; Goodarzi Hosseinabadi, H.; Maharjan, S.; Ruiz-Esparza, G. U.; Khoshakhlagh, P.; Manbachi, A.; Dokmeci, M. R.; Chen, S.; Shin, S. R.; Zhang, Y. S.; Khademhosseini, A., Microfluidics-Enabled Multimaterial Maskless Stereolithographic Bioprinting. *Advanced materials (Deerfield Beach, Fla.)* **2018**, *30* (27), e1800242.
31. Miri, A. K.; Mirzaee, I.; Hassan, S.; Mesbah Oskui, S.; Nieto, D.; Khademhosseini, A.; Zhang, Y. S., Effective bioprinting resolution in tissue model fabrication. *Lab on a chip* **2019**, *19* (11), 2019-2037.
32. Mochizuki, T.; Makabe, S.; Aoyama, Y.; Kataoka, H.; Nitta, K., *New Insights into Cystic Kidney Diseases*. 2018; Vol. 195.
33. Bräuer, P.; Lindner, M.; Studnitzky, T.; Kieback, B.; Rudolph, J.; Werner, R.; Krause, G. In *3D Screen Printing technology — Opportunities to use revolutionary materials and machine designs*, 2012 2nd International Electric Drives Production Conference (EDPC), 15-18 Oct. 2012; 2012; pp 1-5.

34. Panwar, A.; Tan, L. P., Current Status of Bioinks for Micro-Extrusion-Based 3D Bioprinting. *Molecules (Basel, Switzerland)* **2016**, *21* (6), 685.

35. Lee, A.; Hudson, A. R.; Shiawski, D. J.; Tashman, J. W.; Hinton, T. J.; Yerneni, S.; Bliley, J. M.; Campbell, P. G.; Feinberg, A. W., 3D bioprinting of collagen to rebuild components of the human heart. *Science* **2019**, *365* (6452), 482.

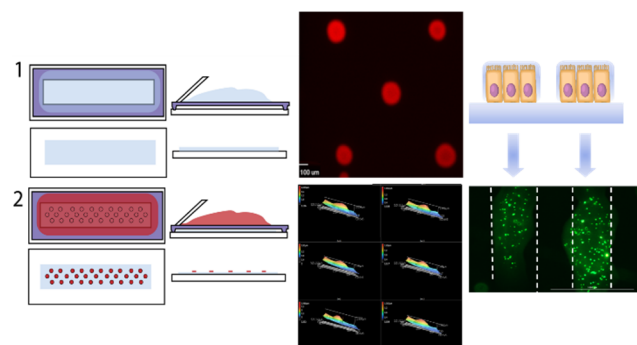
36. Schwartz, R.; Malpica, M.; Thompson, G. L.; Miri, A. K., Cell encapsulation in gelatin bioink impairs 3D bioprinting resolution. *Journal of the mechanical behavior of biomedical materials* **2020**, *103*, 103524.

37. Cao, X.; Chen, H.; Gu, X.; Liu, B.; Wang, W.; Cao, Y.; Wu, F.; Zhou, C., Screen Printing as a Scalable and Low-Cost Approach for Rigid and Flexible Thin-Film Transistors Using Separated Carbon Nanotubes. *ACS nano* **2014**, *8* (12), 12769-12776.

38. Parashkov, R.; Becker, E.; Riedl, T.; Johannes, H.; Kowalsky, W., Large Area Electronics Using Printing Methods. *Proceedings of the IEEE* **2005**, *93* (7), 1321-1329.

39. Bowen, W. P.; Wylie, P. G., Application of laser-scanning fluorescence microplate cytometry in high content screening. *Assay Drug Dev Technol* **2006**, *4* (2), 209-21.

Table of Contents Figure



Screen printing to create 3D tissue models

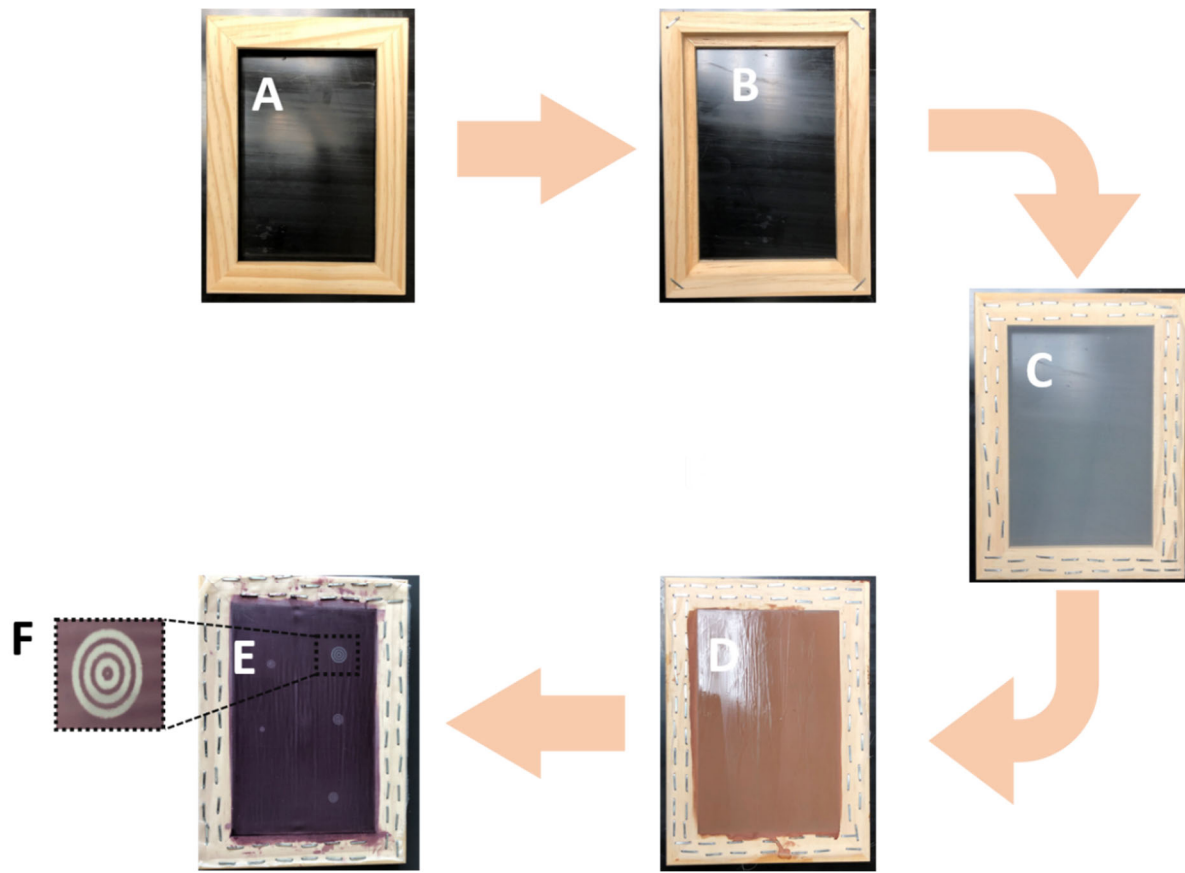
*Narendra Pandala, Sydney Haywood, Michael A. LaScola, Adam Day, Joshua Leckron, Erin Lavik**

Chemical, Biochemical and Environmental Engineering, University of Maryland, Baltimore County, MD 21250, Piscataway Territories

Supplementary Information

Screen Assembly

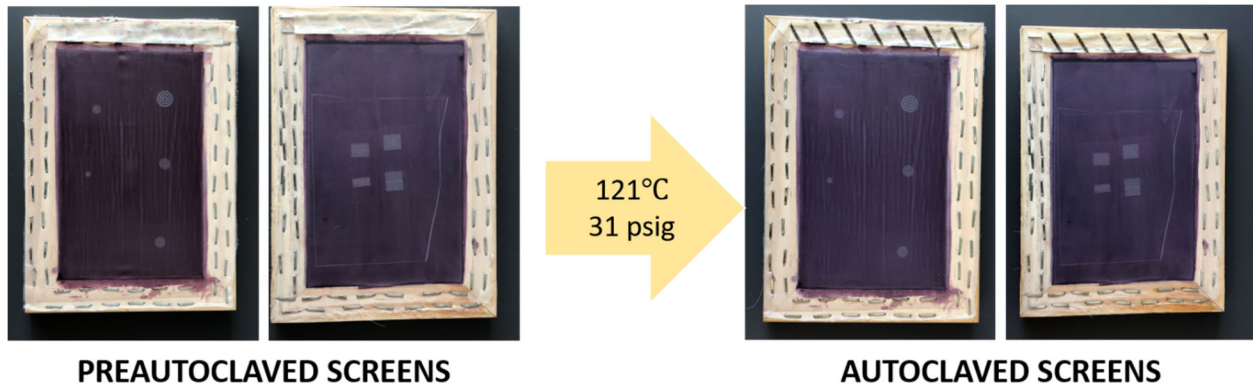
The screen assembly begins with a wooden frame of size 4"x6" (Supplementary Figure -1A). The wooden frame is reinforced using $\frac{1}{4}$ " staples (Arrow T50, USA) to maintain the structural rigidity of the frame in the autoclaving process (Supplementary Figure -1B). A silkscreen of mesh size 125 μ m (43T, 110US) is then stretched on to the wooden frame and then attached to the frame using the $\frac{1}{4}$ " staples (Supplementary Figure -1C). The empty screen is then cleaned using 70% ethanol solution to degrease the mesh. The emulsion (Ulano-925WR-P) is then sensitized (according to the manufactures instructions) by dissolving the sensitizer in the water and mixing it in the emulsion thoroughly until an emulsion of uniform color is obtained. The emulsion is then let to set for an hour, the sensitized emulsion can be stored in dark place at room temperature for 2 months. The emulsion is then coated on to the mesh (Supplementary Figure -1D). The emulsion coated screen is dried overnight in a dark place. The photomasks are designed in Adobe illustrator with the accurate pixel density corresponding to the scale and the printer resolution. The photomasks are then printed on to a transparent OHP sheet using saturated black. The photomasks are then placed on dried emulsion coated screens at approximately 15cm away from a UV lamp (Black-Ray, UVP B100, 365 nm) for 3-5 minutes. The photomask is then removed, and the screens are washed using a stream of water until the non-hardened emulsion from the patterns is completely washed away, the screens are then set to dry (Supplementary Figure -1E). The screens are then placed in an autoclave bag and sterilized to be using in a tissue culture hood. Once the screens are used to print, the screens are washed with water, dried and autoclaved to be reused.



Supplementary Figure 1: A) Empty wooden screen B) wooden frame reinforced with staples C) Silkscreen stretched and attached to the wooden frame D) sensitized emulsion coated screen E) Assembled screen with a concentric circle pattern of various sizes.

Sterilizing the screens:

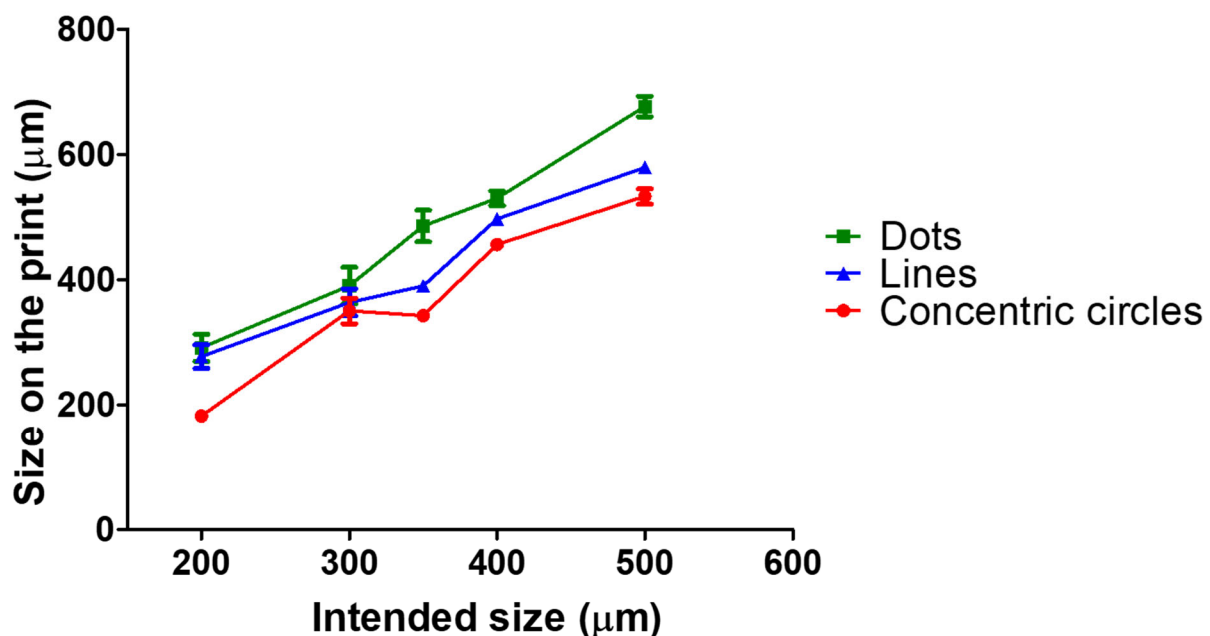
To sterilize the screens and to make them suitable for use in a tissue culture hood, we assembled the screens using wooden frames reinforced with $\frac{1}{4}$ " staples (Arrow T50, USA). The completely assembled and photomasked screens are autoclaved at a temperature of 121°C and a pressure of 31Psig for 15 minutes and 2 minutes of dry time (Gravity-1 setting) in an autoclave. Supplementary Figure 1 shows the images of the screens pre and post autoclave cycle, the screens remained structurally intact, and the pattern on the mesh and the mesh itself maintained its tension, making them suitable for printing after the autoclave cycle. This shows that after each print, the screens can be cleaned and then sterilized using an autoclave making them suitable for aseptic use.



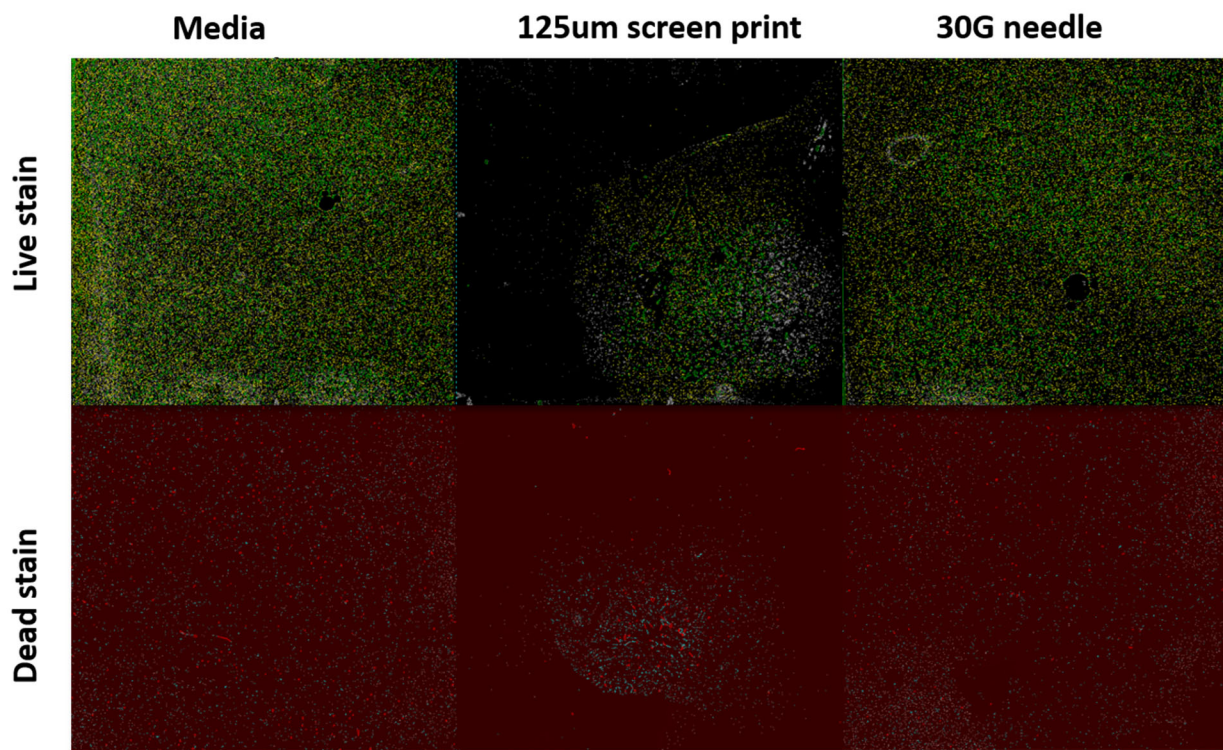
Supplementary Figure 2: Pre and post autoclaved screens, showing autoclaving the screens doesn't alter their structural integrity, making them suitable for integration in an aseptic process

Size of the prints on the transparent sheets:

In the initial stages of the screen printing the patterns are designed on Adobe Illustrator and then printed on to inkjet printer compatible OHP sheets using an inkjet printer (Epson, WF-3640). The size of the patterns on the transparent sheets are measured using the laser confocal scanning microscope VK-X1000 (Keyence, Japan) and the results are analyzed using the Multifile analyzer software (Keyence, Japan). Supplementary Figure 2 shows the size of the patterns on the OHP sheets. From this it can be observed that the inkjet printer results in a size variation of about 70 μm in comparison to the designed pattern, which is carried on to the later stages of the printing process leading to a variation of approximately 90 μm in the size of the prints. This can be adjusted by changing the size of the patterns in the Illustrator and then printing them to adjust for the variation in the sizes on the transparent sheets and there by adjusting the size of the patterns on the screens and finally the size of the prints.



Supplementary Figure 3: Sizes of lines, dots and concentric circles printed on the transparent sheet, showing an increase in size of the prints, which is translated into the later parts of screen assembly (photomasking) and thereby effecting the sizes of the hydrogel prints



Supplementary Figure-4: Virtual images of Live/Dead scans of the Caco-2 cells printed using the screen printing techniques with a (125 μ m mesh size of screen along with a control and 30G needle.

AUTHOR INFORMATION

*** Corresponding Author**

Erin Lavik

Email: elavik@umbc.edu